Mechanics Research Communications 103 (2020) 103477

Contents lists available at ScienceDirect

Mechanics Research Communications

journal homepage: www.elsevier.com/locate/mechrescom

Design of minimal mass load-bearing tensegrity lattices

Raman Goyal[a], Robert E. Skelton[a], Edwin A. Peraza Hernandez[b,*]

[a] Department of Aerospace Engineering, Texas A&M University, College Station, TX 77843-3141, USA
[b] Department of Mechanical and Aerospace Engineering, University of California, Irvine, Irvine, CA 92697-3975, USA

ARTICLE INFO

Article history:
Received 31 August 2019
Revised 8 January 2020
Accepted 9 January 2020
Available online 18 January 2020

Keywords:
Lattice Materials
Compressive Structures
Tensegrity
Lightweight Structures

ABSTRACT

Lattice metamaterials have demonstrated promising characteristics such as having tunable/unconventional properties and being lightweight. This work centers on the design of tensegrity-based lattices, known as "T-bar" structures, capable of supporting compressive loads with minimum mass. Analytical formulas for the calculation of the mass of these structures under externally applied forces and pre-stress are derived. These formulas account for local failure of the T-bar structures (material yielding and buckling of its individual members). A numerical approach is introduced to assess the global stability of the structures under external forces and pre-stress and to account for global buckling in the design process. The mass of the structure is minimized by adjusting its shape and topology while global buckling is simultaneously prevented using two different design methods: *i)* optimizing the pre-stress distribution in the structure, and *ii)* optimizing the cross-section areas of the tensegrity members. Using either method, the results show that 2D and 3D T-bars possess a global minimum mass design for a given externally applied force and length. The computed results also show that designs obtained by optimizing the cross-section areas of the members have lower mass than those obtained by optimizing the pre-stress distribution.

© 2020 Elsevier Ltd. All rights reserved.

1. Introduction

Lattice metamaterials are currently being investigated for their attractive engineering properties including negative or tunable Poisson's ratio [1,2], improved thermal resistance [3], tunable thermal expansion [4,5], load-bearing capabilities with low mass density [6], and high energy absorption and tunable energy dissipation [7,8]. A key challenge in the development of lattice metamaterials is to determine the most favorable arrangement of matter (the lattice members) to achieve a target property. The theory of *tensegrity* structures (pre-stressable trusses with compression and tension-only members [9]) can provide solutions to the design of lattice materials. For example, Fraternali and coworkers demonstrated tunable acoustic properties in tensegrity-based metamaterials [10]. Also, Zhang and coworkers designed and fabricated tensegrity metamaterials with high energy absorption [11].

An important property of tensegrity structures that can be exploited in lattice materials is their ability to support loads with minimum mass. Tensegrities having a double-pyramid form known as D-bars have been theoretically shown to support compressive forces and absorb energy with minimum mass [12,13]. Other examples include the tensegrity "Michell truss" that has been analytically demonstrated to support cantilever-type loads with minimal mass [14], and tensegrity tori that support concentric loads with minimum mass [15].

The objective of this work is to design tensegrity lattices for the support of compressive loads with minimal mass. The focus is on a tensegrity topology known as the T-bar structure, previously studied and proposed for compressive constructions [16,17]. Schematics of T-bar structures are shown in Fig. 1. These structures have double-pyramid shape and compressive forces applied at their end points. T-bars can be used as components of lightweight lattice materials as illustrated in Fig 1. A T-bar of complexity $q = 1$ is formed by a single *T-bar unit* that has two bars (compressive members) of equal length along the loading direction and p bars connecting the intersection of the longitudinal bars to the vertices of a centered p-sided regular polygon. Fig. 1 shows T-bars of $p = 2$ (2D T-bars) and $p = 4$ (T-bars with a centered square). Strings (tensile members) form the sides of the central polygon and also connect the vertices of this polygon to the end points of the T-bar unit. A T-bar of complexity q is formed by replacing the longitudinal bars of a T-bar of complexity $q - 1$ with T-bar units (this is denoted as a self-similar iteration), as illustrated in Fig. 1 for T-bars of complexities $q = 2$ and $q = 3$.

The contributions of this work are summarized as follows:

- This work presents, for the first time, a formulation to perform minimal mass design of compressive 2D *and* 3D T-bar

* Corresponding author.
E-mail address: eperazah@uci.edu (E.A. Peraza Hernandez).

https://doi.org/10.1016/j.mechrescom.2020.103477
0093-6413/© 2020 Elsevier Ltd. All rights reserved.

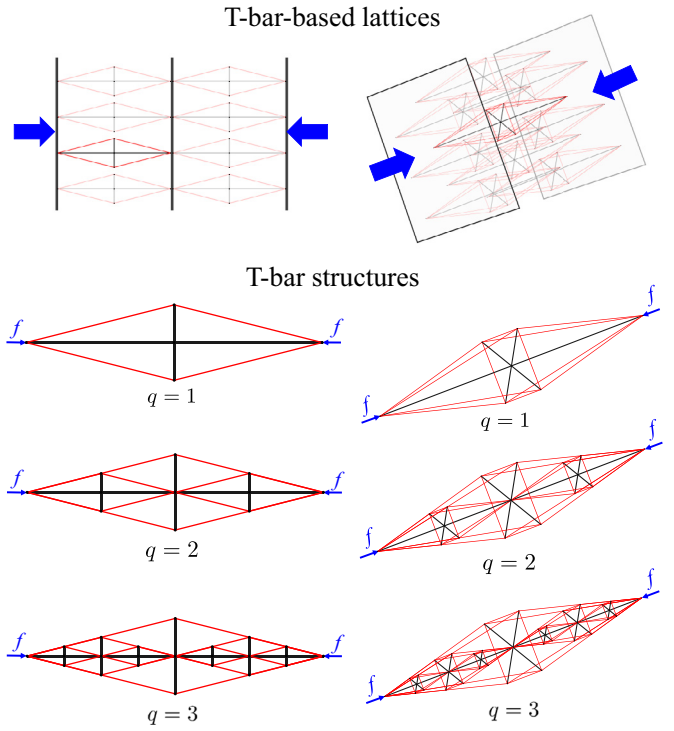

Fig. 1. 2D and 3D T-bar structures of different complexity q. These structures can be integrated in larger assemblies to synthesize lattice compressive materials of minimal mass.

lattices of *arbitrary complexity*. Previous studies of T-bar compressive structures have only considered T-bars of complexity $q = 1$ [17] or are limited to 2D T-bars [16].

- Equations for the loads in bars and strings of T-bar systems are extended from previous works [12,16] to account for *arbitrary pre-stress loading scenarios*.
- A novel algorithm that allows for the design of minimum mass 2D and 3D T-bars of any complexity is developed. Local and global failure stability constraints are concurrently accounted for in the minimal mass design of T-bar systems. Two approaches for the prevention of global instabilities are implemented in the algorithm: one based on optimizing the pre-stress distribution and the other on optimizing the cross-section areas of the members. The algorithm hierarchically determines minimal mass designs of the T-bar units introduced at each self-similar iteration and hence the final T-bar system is also of minimal mass.

The design of compressive T-bar members of minimal mass is relevant for the development of any general tensegrity structure where *lightweight properties* are critical. This is because monolithic compressive members (bars or struts) can be replaced with T-bars of optimal complexity to minimize the overall structural mass. Examples of recent practical tensegrity structures that would greatly benefit from the replacement of bars/struts by optimal T-bars include: metamaterials based on pentamode lattices studied by Fraternali and coworkers [18,19]; ball-like robots for planetary exploration investigated by Sunspiral and coworkers [20,21]; and minimal mass tensegrity bridges researched by Fraternali and coworkers [22,23].

2. Minimum mass under local failure constraints

This section provides the analytical formulas for the mass of T-bar structures considering local failure criteria of the individual

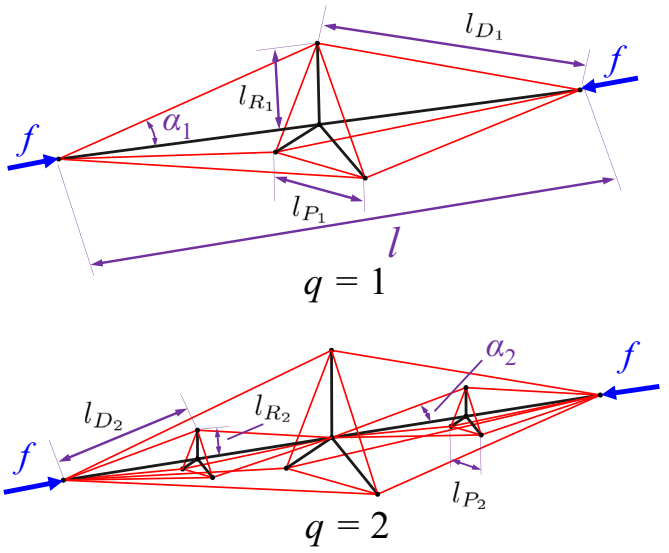

Fig. 2. Geometric parameters of 3D tensegrity T-bar systems for complexities $q = 1, 2$.

members. Fig. 2 shows a 3D T-bar structure subjected to a compressive force f. The total length of the T-bar structure, is denoted by l. Each T-bar unit forming a T-bar structure has two kinds of bars: *longitudinal bars* that are aligned with the applied compressive force, and *radial bars* that connect the center of the unit to the vertices of the central polygon. A T-bar unit also has two kinds of strings: *planar strings* that form the sides of the central polygon and *diagonal strings* that connect the vertices of the central polygon to the end points of the unit. In each T-bar unit, the angle between the longitudinal bars and the diagonal strings is denoted as the aperture angle. The aperture angle of the T-bar units introduced at the ith self-similar iteration is denoted by α_i, where $i = 1, 2, \ldots, q$ (see Fig. 2).

The material properties of the bars and strings are assumed given, and therefore the calculation of the mass of the T-bar consists of finding the cross-section area (obtained through local failure constraints) and the length of the members. The length of the longitudinal bars, radial bars, diagonal strings, and planar strings are denoted by l_L, l_{R_i}, l_{D_i}, and l_{P_i}, respectively. Also, the total number of longitudinal bars, radial bars, diagonal strings, and planar strings in the T-bar structure are denoted by n_L, n_{R_i}, n_{D_i}, and n_{P_i}, respectively, for $i = 1, \ldots, q$. These parameters are determined from geometry as follows:

$$n_L = 2^q, \quad l_L = \frac{l}{2^q}. \tag{1}$$

$$n_{R_i} = 2^{i-1}(p), \quad l_{R_i} = \frac{l}{2^i}\tan(\alpha_i), \quad \text{for} \quad i = 1, 2, \ldots, q, \tag{2}$$

$$n_{D_i} = 2^{i-1}(2p), \quad l_{D_i} = \frac{l}{2^i \cos(\alpha_i)}, \quad \text{for} \quad i = 1, 2, \ldots, q, \tag{3}$$

$$n_{P_i} = 2^{i-1}(p), \quad l_{P_i} = \frac{2l \sin\left(\frac{\pi}{p}\right)\sin(\alpha_i)}{2^i \cos(\alpha_i)}, \quad \text{for } i = 1, 2, \ldots, q. \tag{4}$$

The magnitude of compressive force in the radial bars introduced at each iteration is denoted by f_{R_i}, $i = 1, \ldots, q$, and the magnitude of the compressive force in the longitudinal bars is denoted by f_L. Using the static equilibrium condition that the sum of the member forces at each node is zero, the magnitude of compressive forces in all the bar members can be uniquely calculated from the

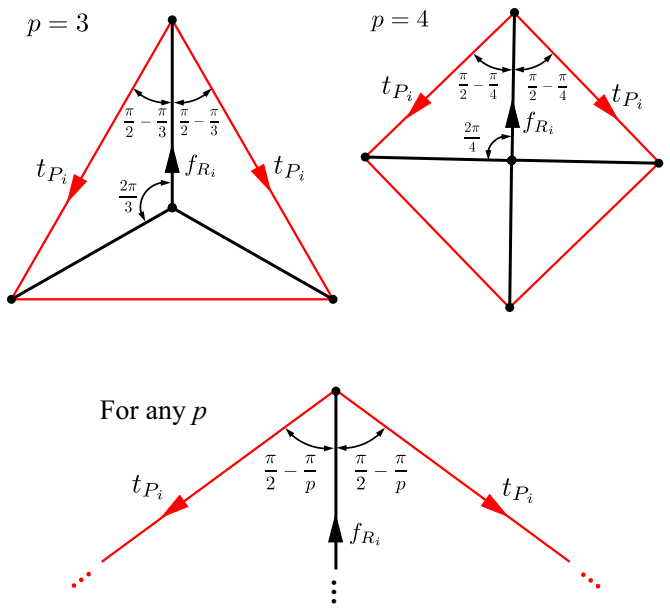

Fig. 3. Force balance diagram for planar strings and radial bars. These schematics illustrate the central p-sided polygon of a T-bar unit.

given external force f and independent string pre-tensions t_{D_i} and t_{P_i}:

$$f_L = f + p\sum_{i=1}^{q} t_{D_i}\cos(\alpha_i), \quad f_{R_i} = 2t_{D_i}\sin(\alpha_i) + 2t_{P_i}\sin\left(\tfrac{\pi}{p}\right), \quad \text{for} \quad i = 1, 2, \ldots, q. \tag{5}$$

The term $2t_{P_i}\sin\left(\frac{\pi}{p}\right)$ in the formula for the compressive force of the radial bars f_{R_i} in Eq. (5) can be intuitively observed by analyzing the force balance of the central p-sided polygon of a T-bar unit. Examples for $p = 3$, $p = 4$, and any p are provided in Fig. 3. These schematics indicate that the radial bars must balance a force of $t_{P_i}\cos\left(\frac{\pi}{2} - \frac{\pi}{p}\right)$ for each of the two planar strings connected at every polygon vertex, making the total force contribution of these strings into the compressive force of the radial bars $2t_{P_i}\cos\left(\frac{\pi}{2} - \frac{\pi}{p}\right) = 2t_{P_i}\sin\left(\frac{\pi}{p}\right)$.

Note that t_{D_i} and t_{P_i} are pre-tensions that can be arbitrarily selected to adjust the load distribution in a T-bar. Eq. (5) is valid for any $p \geq 2$, $q \geq 1$, and $\alpha_i > 0$. Using Euler theory of buckling, the minimum mass of a compressive member of length $\hat{l}$ subjected to a force $\hat{f}$ that is designed to satisfy buckling constraints is given as [13]:

$$m_{bB} = 2\rho_b\hat{l}^2\left(\frac{\hat{f}}{\pi E_b}\right)^{\frac{1}{2}}, \tag{6}$$

where ρ_b and E_b are the mass density and Young's modulus of the bar material, respectively. The minimum mass of a compressive member designed under yielding constraint is denoted by m_{bY} and the minimum mass of a tensile member also designed under yielding constraint is denoted by m_{sY}. These are given by:

$$m_{bY} = \frac{\rho_b}{\sigma_b}\hat{l}\hat{f}, \quad m_{sY} = \frac{\rho_s}{\sigma_s}\hat{l}\hat{f}, \tag{7}$$

where σ_b is the yield stress of the bar material and ρ_s and σ_s are the mass density and yield stress of the string material. The minimum mass of a compressive member is the maximum of the mass required for either yielding or buckling constraints, while a tensile member is only subjected to yield constraints. Accordingly, the mass of a string m_s and the mass of a bar m_b of a T-bar structure are:

$$m_b = \max(m_{bB}, m_{bY}), \quad m_s = m_{sY}. \tag{8}$$

The minimum mass of the string and bar members in a T-bar structure are obtained by substituting the force and length values from Eqs. (2)-(5) into Eqs. (6)-(8). Then, the minimum total mass of a T-bar system subjected to a compressive force of magnitude f is obtained as the addition of the mass of all the members in the system as:

$$m_T = \max(m_{LB}, m_{LY}) + \sum_{i=1}^{q}\max\left(m_{RB_i}, m_{RY_i}\right) + \sum_{i=1}^{q} m_{P_i} + \sum_{i=1}^{q} m_{D_i}, \tag{9}$$

where the mass of the different kinds of members is:

$$m_{LB} = \frac{2\rho_b l^2}{\sqrt{\pi E_b}}\frac{\sqrt{f + p\sum_{i=1}^{q} t_{D_i}\cos(\alpha_i)}}{2^q}, \tag{10}$$

$$m_{LY} = \frac{\rho_b}{\sigma_b} l\left(f + p\sum_{i=1}^{q} t_{D_i}\cos(\alpha_i)\right), \tag{11}$$

$$m_{RB_i} = \frac{2\rho_b l^2}{\sqrt{\pi E_b}}\frac{p\tan^2(\alpha_i)\sqrt{2t_{D_i}\sin(\alpha_i) + 2t_{P_i}\sin\left(\frac{\pi}{p}\right)}}{2^{i+1}}, \tag{12}$$

$$m_{RY_i} = \frac{\rho_b}{\sigma_b} pl\tan(\alpha_i)\left(t_{D_i}\sin(\alpha_i) + t_{P_i}\sin\left(\tfrac{\pi}{p}\right)\right), \tag{13}$$

$$m_{P_i} = \frac{p\rho_s l\sin\left(\frac{\pi}{p}\right)\sin(\alpha_i)}{\sigma_s\cos(\alpha_i)} t_{P_i}, \quad m_{D_i} = \frac{p\rho_s l}{\sigma_s\cos(\alpha_i)} t_{D_i}. \tag{14}$$

This section provided the minimum mass (Eq. (9)) for a T-bar structure for given pre-stress in the strings t_{P_i} and t_{D_i} and externally applied compressive force f. Only local failure modes of the individual members in the T-bar structure were considered. The next section provides the formulation employed to assess the global buckling properties of T-bar tensegrity structures to also account for such failure mode in the structural design.

3. Global buckling analysis

A T-bar structure subjected to an external compressive force and pre-stress can lose its load-bearing capability due to both local and global failure modes. Global failure in this context entails buckling of the T-bar structure as a whole without necessarily reaching the load level required for local failure of its individual members. This section presents the formulation that allows for the design of the pre-tensions in the strings and the cross-section areas of the members required to prevent global buckling.

3.1. Stiffness matrix formulation

The global stiffness matrix of the entire T-bar structure is determined from the contributions of the stiffness matrices from all its individual members. A recent paper [24] provided the derivation for the linearized global stiffness matrix which can be obtained by linearizing the static equilibrium equation of tensegrity structures given as [25]:

$$S\hat{\gamma}C_s - B\hat{\lambda}C_b = W, \tag{15}$$

where $S = [s_1\ s_2\ \cdots\ s_\tau]$ and $B = [b_1\ b_2\ \cdots\ b_\beta]$ are the matrices containing the vectors along the lengths of the strings s_j and bars b_k, respectively. The total number of strings in the T-bar is denoted by τ and the total number of bars is denoted by β. The force density (magnitude of the tensile force per unit length) in the jth string is denoted by $\gamma_j \geq 0$ and the force density (the magnitude

of the compressive force per unit length) in the kth bar is denoted by $\lambda_k \geq 0$. The string connectivity matrix C_s and bar connectivity matrix C_b provide the information of the start and end nodes of each string and each bar, respectively [25]. The diagonal matrices $\hat{\gamma}$ and $\hat{\lambda}$ are written by arranging γ_j and λ_k in their diagonal elements, and the external force matrix $W = [w_1\ w_2\ \cdots\ w_\nu]$ contains the vector of external forces w_i applied to the ith node. The number of nodes in the system is denoted by ν.

The non-linear static equilibrium Eq. (15) is linearized about an equilibrium configuration to obtain:

$$\mathbb{K}_L \mathrm{d}n = \mathrm{d}w, \tag{16}$$

where $\mathrm{d}n = [\mathrm{d}n_1^\top\ \mathrm{d}n_2^\top\ \cdots\ \mathrm{d}n_\nu^\top]^\top$ is a vector containing small variations of the node positions vectors, and $\mathrm{d}w = [\mathrm{d}w_1^\top\ \mathrm{d}w_2^\top\ \cdots\ \mathrm{d}w_\nu^\top]^\top$ is a vector containing small variations of external forces at all the nodes. The linearized global stiffness matrix $\mathbb{K}_L$ from Eq. (16) is given as [24]:

$$\begin{aligned}\mathbb{K}_L = {} & (C_s^\top \otimes I_3)\,\mathrm{b.d.}(\cdots, K_{s_j}, \cdots)(C_s \otimes I_3) \\ & -(C_b^\top \otimes I_3)\,\mathrm{b.d.}(\cdots, K_{b_k}, \cdots)(C_b \otimes I_3).\end{aligned} \tag{17}$$

The contributions of the jth string and the kth bar in the global stiffness matrix are denoted by K_{s_j} and K_{b_k}, respectively:

$$K_{s_j} \triangleq \gamma_j I_3 + E_{s_j} A_{s_j} \frac{s_j s_j^\top}{l_{s_j}^3}, \quad K_{b_k} \triangleq \lambda_k I_3 - E_{b_k} A_{b_k} \frac{b_k b_k^\top}{l_{b_k}^3}, \tag{18}$$

where E_{s_j} and A_{s_j} are the Young's modulus and the cross-section area of the jth string, respectively. Similarly, E_{b_k} and A_{b_k} denote the Young's modulus and the cross-section area of the kth bar member.

3.2. Criteria for global stability of T-bar structures

The string force density vector $\gamma = [\gamma_1\ \gamma_2\ \cdots\ \gamma_\tau]^\top$ and the bar force density vector $\lambda = [\lambda_1\ \lambda_2\ \cdots\ \lambda_\beta]^\top$ can be written as the sum of force densities due to pre-stress (γ_p, λ_p) and force densities due to the external force (γ_w, λ_w) as:

$$\gamma = \gamma_p + \gamma_w, \quad \lambda = \lambda_p + \lambda_w, \tag{19}$$

where the force densities due to pre-stress (self-equilibrated under zero external force) are solved using the static equilibrium equation (Eq. (15)) as:

$$(C_b^\top \otimes I_3)\hat{B}\lambda_p = (C_s^\top \otimes I_3)\hat{S}\gamma_p, \quad \gamma_p \geq 0, \quad \lambda_p \geq 0, \tag{20}$$

where I_3 is the identity matrix of dimension 3×3 and $\hat{S} = \mathrm{b.d.}(s_1, s_2, \ldots, s_\tau)$ and $\hat{B} = \mathrm{b.d.}(b_1, b_2, \ldots, b_\beta)$ are the body diagonal matrices formed by arranging the string vectors s_j and bar vectors b_k along their body diagonals, respectively. Eq. (20) gives a unique solution for the force densities in the bars (λ_p) for given values of pre-stress in the strings (γ_p) because the coefficient matrix $(C_b^\top \otimes I_3)\hat{B}$ is a full column rank matrix for any T-bar structure. This can also be confirmed from the exact analytical solution given in Eq. (5).

The external force f on the T-bar structure only causes compressive loading in the longitudinal bars. This can be verified from Fig. 2 and Eq. (5):

$$\gamma_w = 0, \quad \lambda_{w_k} = \begin{cases} \frac{2^q f}{l}; & \text{For longitudinal bars} \\ 0; & \text{Otherwise} \end{cases}. \tag{21}$$

Using Eqs. (20) and (21), the linearized global stiffness matrix from Eq. (17) is updated with:

$$K_{s_j} = \gamma_{p_j} I_3 + E_{s_j} A_{s_j} \frac{s_j s_j^\top}{l_{s_j}^3}, \tag{22}$$

$$K_{b_k} = (\lambda_{p_k} + \lambda_{w_k}) I_3 - E_{b_k} A_{b_k} \frac{b_k b_k^\top}{l_{b_k}^3}. \tag{23}$$

From Eq. (16), global instability is interpreted as non-trivial values of displacement in the structure ($\mathrm{d}n \neq 0$) under no changes in the values of the external forces ($\mathrm{d}w = 0$):

$$\mathbb{K}_L \mathrm{d}n = 0. \tag{24}$$

Eq. (24) has non-trivial solutions for dn, *if and only if*, the symmetric global stiffness matrix $\mathbb{K}_L$ is singular, or determinant of $\mathbb{K}_L$ is zero. Thus, to minimize mass of the T-bar structure under global instability constraints, the minimum values of pre-stress (γ_p) or cross-section areas of the members such that the matrix $\mathbb{K}_L$ reaches singularity (*i.e.,* the onset of buckling failure) for the given external force f must be determined.

As stated in Eq. (24), global stability of the tensegrity structures is assessed by means of a linearized matrix, as in buckling analysis of beams and plates using the finite element method [26,27]. This matrix is obtained by linearizing the non-linear equations of static equilibrium (Eq. (15)) about the current equilibrium configuration of the tensegrity structure. Some inaccuracy is introduced in the process as here the nominal (initial) coordinate positions of the nodes are employed instead of their deformed positions. However, such differences in node positions between initial and deformed configurations are small as the strings and bars are assumed to be comprised of a stiff material in this work (aluminum). Thus, changes in the length of the strings and bars, and consequently differences in node positions between initial and deformed configurations, are small compared to the dimensions of the tensegrity. Further research quantifying the effect of this assumption and non-linear buckling analysis of tensegrity structures are recommended for future studies.

The mass minimization of the structure considering global buckling alone is a convex problem (unique optimum solution) as all the design variables appear linearly in Eq. (24). However, the combined problem of minimizing the mass of the structure considering both local and global failure becomes a non-convex as the area of the bar members (A_{b_k}) is a non-linear function of the force densities in the bar λ_k, for local buckling constraints (*cf.* Eq. (6)). The next section discusses two design approaches to solve this non-convex problem.

4. Methods for determining minimum mass designs of T-bar structures

This section describes two approaches to minimize the mass of T-bar structures based on the local and global failure criteria developed in the previous sections.

4.1. Pre-stress method: optimum pre-stress for a T-bar unit

A T-bar unit (equivalent to a T-bar of $q = 1$) has p planar strings and $2p$ number of diagonal strings that can be independently pre-stressed. The tension in these strings is scaled using two independent *pre-stress factors:* $\gamma_P \geq 0$ for planar strings and $\gamma_D \geq 0$ for diagonal strings,

$$\gamma_p = \begin{bmatrix} \gamma_P\,[1\ 1\ \cdots\ 1]_{p\times 1}^\top \\ \gamma_D\,[1\ 1\ \cdots\ 1]_{2p\times 1}^\top \end{bmatrix}. \tag{25}$$

The force density in the bars due to pre-stress (λ_p) can be uniquely calculated as a function of pre-stress factors γ_P and γ_D using Eq. (20). Eq. (19) allows us to solve for the force density in each member and Eqs. (6) and (7) are used to calculate the area of each member. All the variables in Eq. (17) are now dependent on the pre-stress factors. The design problem to minimize the mass of the T-bar unit then consists of finding the minimum values of the pre-stress factors such that the stiffness matrix of the T-bar unit $\mathbb{K}_L$ reaches singularity, which physically represents the onset of global buckling.

4.2. Area method: optimum string cross-section areas for a T-bar unit

Similar to the method discussed in Section 4.1, the cross-section areas of the planar strings and diagonal strings can be independently scaled to prevent global buckling. Let us define $\eta_P \geq 1$ and $\eta_D \geq 1$ as the *area factors* that scale the cross-section areas of the planar strings A_P and diagonal strings A_D, respectively. The areas of the strings are then scaled as follows:

$$A_P \rightarrow \eta_P A_{Pb}, \quad A_D \rightarrow \eta_D A_{Db}, \tag{26}$$

where A_{Pb} and A_{Db} are the baseline member cross-section areas [12]. Pre-stress values of $\gamma_p = \lambda_p = 0$ are used in this method. The design problem for this method consists of finding the minimum values of the area factors such that the stiffness matrix of the T-bar unit $\mathbb{K}_L$ reaches singularity.

4.3. Hierarchical design of T-bar structures

For a T-bar structure of complexity q, there would be different T-bar units introduced at each self-similar iteration that may be subjected to global buckling. The minimum mass design of a T-bar is obtained when the T-bar units introduced at each self-similar iteration are designed such that they reach the onset of buckling. Algorithm 1 outlines the hierarchical design approach for minimal mass T-bar structures of arbitrary complexity, where the pre-stress or area factors of T-bar units are optimized sequentially for each self-similar iteration i, from $i = 1$ to $i = q$.

Algorithm 1: Hierarchical design of minimal mass T-bar structures with arbitrary complexity.

Step 1: Design a complexity $q = 1$ T-bar structure (equivalent to a T-bar unit) of length $l_1 = l$ and external force $f_1 = f$ by determining the minimum values of pre-stress or area factors for both planar and diagonal strings ($[\gamma_{P_1}, \gamma_{D_1}]$ or $[\eta_{P_1}, \eta_{D_1}]$) such that the stiffness matrix of the T-bar unit $\mathbb{K}_{L_1}$ reaches singularity.

Step 2: Design the T-bar units of the subsequent self-similar iteration $i+1$ which have length $l_{i+1} = l/2^i$ and external force $f_{i+1} = f_i + p\,\gamma_{D_i}\, l_{D_i} \cos(\alpha_i)$ by calculating the minimum pre-stress or area factors ($[\gamma_{P_{i+1}}, \gamma_{D_{i+1}}]$ or $[\eta_{P_{i+1}}, \eta_{D_{i+1}}]$) such that the stiffness matrix of the T-bar units $\mathbb{K}_{L_{i+1}}$ reaches singularity.

Step 3: Repeat **Step 2** for each self-similar iteration.

5. Results and discussion

Results of mass minimization for 2D and 3D T-bar structures using the approach developed in the previous section are presented herein. The *mass ratio* μ is used to compare the mass of the T-bar structures m_T with that of a compressive column of solid circular cross-section, m_{col}, as:

$$\mu = \frac{m_T}{m_{col}}, \quad \text{where} \quad m_{col} = \max\left(\frac{2\rho_b l^2\sqrt{f}}{\sqrt{\pi E_b}}, \frac{\rho_b l f}{\sigma_b}\right). \tag{27}$$

If $\mu < 1$, the T-bar structure requires less mass than the compressive column to support a compressive force f. Note that both yielding and buckling failure modes are accounted for in the mass calculation of the solid column. The mass ratio is referred to as μ_{2D} for 2D T-bars and μ_{3D} for 3D T-bars.

The increase in pre-stress and cross-section area required to prevent global buckling of a T-bar system under compressive loading (obtained via the pre-stress and area methods, respectively) add mass to the structure. To quantify this additional mass, a parameter ϕ defined as the ratio of the mass of the T-bar designed considering global buckling m_T and the mass of the T-bar designed without considering global buckling $m_{T_{local}}$ is introduced:

$$\phi = \frac{m_T}{m_{T_{local}}}, \tag{28}$$

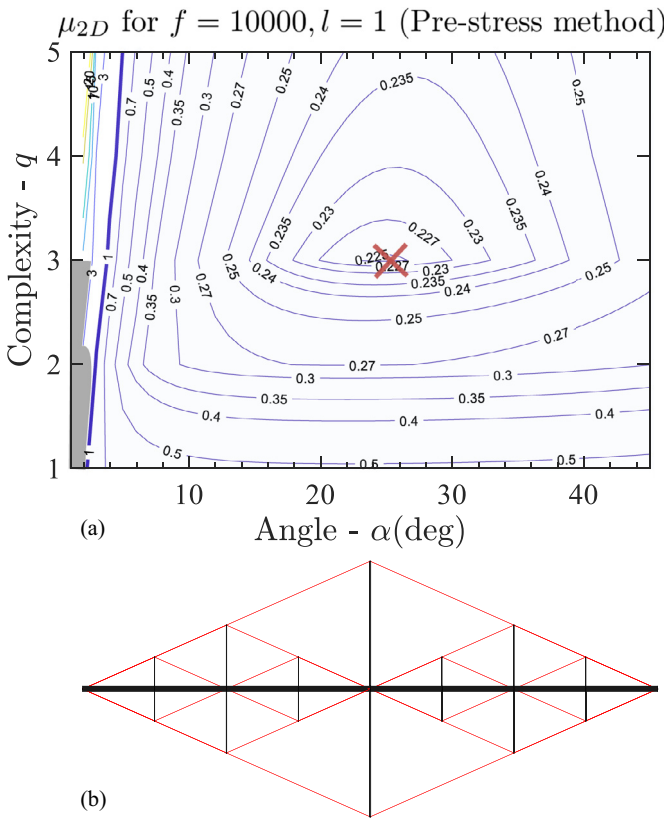

Fig. 4. (a) Contour plot of mass ratio μ_{2D} for 2D T-bar structures with optimized pre-stress factor (γ_D). (b) Minimal mass configuration of the T-bar structure (marked with the ' × ' in the contour) displaying calculated member cross-sections.

where $m_{T_{local}}$ is calculated using Eq. (9) with $t_{D_i} = t_{P_i} = 0$ to consider only local failure constraints. This parameter is referred to as ϕ_{2D} for 2D T-bars and ϕ_{3D} for 3D T-bars.

Material properties of aluminum are used for both string and bar members ($E_s = E_b = 60$ GPa, $\sigma_s = \sigma_b = 110$ MPa, and $\rho_s = \rho_b = 2700$ kg/m^3) and the analogous compressive column. For simplicity, it is assumed that the aperture angles of the T-bar units are equal among all the self-similar iterations: $\alpha_1 = \alpha_2 = \cdots = \alpha_q = \alpha$.

5.1. 2D T-bar structures

For 2D T-bar structures ($p = 2$), there are no planar strings and thus the only optimization variables are the pre-stress factor (γ_D) and the area factor (η_D). Fig. 4(a) provides the contour plots of the mass ratio μ_{2D} for a 2D T-bar structure for pre-stress factor γ_D obtained using Algorithm 1. The lighter shaded area in the contour plot corresponds to the region where the mass of the T-bar structure is lower than the mass of a compressive column designed for buckling $m_T < m_{col}$. As observed in the figure, T-bar structures provide lower mass solutions for compressive loads for a large range of aperture angles and throughout the entire studied complexity range ($q = 1, \ldots, 5$). The darker shaded region in the contour plot represents the complexity and angle set (q, α) where global buckling cannot be prevented for any value of pre-stress in the strings. This can be explained as T-bar structures of low aperture angles have a large "length-to-width" ratio and thus have low critical buckling forces. Fig. 4(a) also shows that there is a global optimum design for the given force f and length l, which was found to be $\mu_{2D} = 0.2246$ for $q = 3$ and $\alpha = 24^\circ$ (marked with an ' × ' in the contour plot). Fig. 4(b) shows the optimum configuration of the T-bar structure displaying the calculated member cross-sections.

Table 1
Mass ratio μ_{2D} optimized with two different methods for different values of force f and length l. Units: f (N), l (m), and α (deg).

$\frac{f}{l^2}$	f	l	Pre-stress method				Area method			
			q	α	μ_{2D}	ϕ_{2D}	q	α	μ_{2D}	ϕ_{2D}
1000	1000	1	4	20	0.08	1.28	4	26	0.07	1.12
2500	2500	1	4	22	0.12	1.81	4	29	0.10	1.51
10000	10000	1	3	24	0.22	1.66	3	31	0.21	1.58
100000	1000	0.1	1	28	0.65	1.30	1	33	0.63	1.26
250000	2500	0.1	1	31	1.01	1.53	1	33	1.00	1.51
1000000	10000	0.1	1	35	1.52	1.52	1	33	1.51	1.51

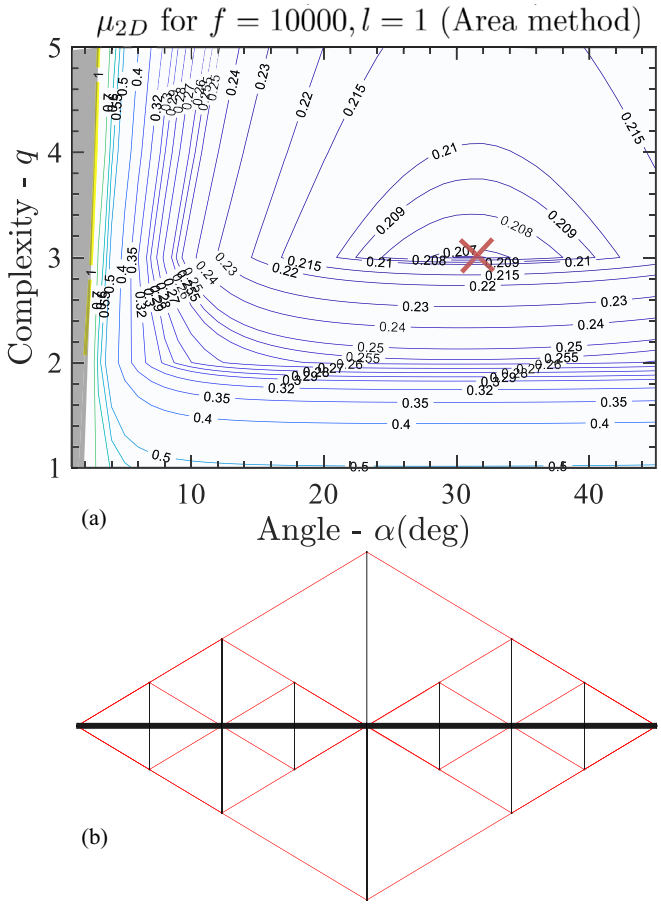

Fig. 5. (a) Contour plots of mass ratio μ_{2D} for the 2D T-bar structure with optimized area factor (η_D). (b) Optimum configuration of the T-bar structure (marked with the ' × ' in the contour) displaying calculated member cross-sections.

The contour plots of mass ratio μ_{2D} for optimized area factor η_D are shown in Fig. 5(a) and the global optimum configuration ($q = 3, \alpha = 31^\circ, \mu_{2D} = 0.2068$) is shown in Fig. 5(b). Notice that the method of optimizing area factor (η_D) provides a solution with lower mass than that obtained by optimizing the pre-stress factor (γ_D). The same trend is observed for different values of f and l as shown in Table 1.

Table 1 also provides optimum complexity q and angle α for different combinations of force f and length l. The first column in the table represents a force per unit area parameter f/l^2. For a small value of this parameter, the compressive column is more prone to buckling failure and thus the mass ratio μ_{2D} is small (more mass savings by replacing the column with a T-bar). The value of the mass ratio increases with the increased value of the parameter f/l^2 and for $f/l^2 = 250000$ N/m^2 the mass ratio is greater than 1 ($\mu_{2D}(\gamma_D) = 1.0157 > 1$, $\mu_{2D}(\eta_D) = 1.0015 > 1$) for both methods indicating that the single column is the minimum mass structure. Notice that for $f/l^2 = 1000000$ N/m^2, the single column is designed to avoid yielding failure and thus the mass of T-bar designed to avoid only local failures would be equal to the mass of the single column, $m_{T_{local}} = m_{col}$. Thus, the reason for the mass ratios $\mu_{2D} = 1.52$ (pre-stress method) and $\mu_{2D} = 1.51$ (area method) to be above 1 is entirely based on global stability to the structure, hence $\mu_{2D} = \phi_{2D} = 1.52$ (pre-stress method) and $\mu_{2D} = \phi_{2D} = 1.51$ (area method).

By comparing the results between the *pre-stress method* and the *area method* in Figs. 4 and 5, and Table 1, one observes that the two methods provide different minimal mass designs under the same loading and length requirements. Cross-section area A_{s_j} and member force $t_{s_j} = \gamma_j \|s_j\|$ are linearly related for tensile string members under yielding failure constraints through the equation $\sigma_s A_{s_j} = t_{s_j}$. For compressive bars under buckling failure constraints, the cross-section area A_{b_k} and member force $f_{b_k} = \lambda_k \|b_k\|$ are non-linearly related through the Euler buckling formula $(\pi E_b A_{b_k}^2)/(4\|b_k\|^2) = f_{b_k}$. In a T-bar structure, increasing tension in the strings increases the compressive forces in the bars and thus the area/mass of the bar members is non-linearly increased. Because of this, increasing the pre-stress in the T-bar structure (which increases the areas of strings and bars accordingly) in the *pre-stress method*; and only increasing the cross-section areas of the strings (without adding pre-stress) in the *area method*, provide different minimal mass results to prevent global buckling.

5.2. 3D T-bar structures

For 3D T-bar structures, we have to simultaneously consider the two pre-stress factors γ_P and γ_D for the pre-stress method and the two area factors η_P and η_D for the area method. It was found that the pre-stress of the planar strings γ_P is not a critical parameter to prevent global buckling and to minimize the mass of the structure. As such, this pre-stress value is kept at $\gamma_P = 10$ for the remainder of these examples. A contour plot of mass ratio μ_{3D} for optimized pre-stress factor (γ_D) as shown in Fig. 6(a). The global optimum configuration (marked with an ' × ') was found to be $q = 3$ and $\alpha = 25^\circ$ with a mass ratio of $\mu_{3D} = 0.2500$. The darker shaded area in the figure corresponds to the region where no solution for γ_D was found to prevent global buckling. Fig. 6(b) shows the optimum configuration of the T-bar structure.

It was also observed for the area method that the cross-section areas of the planar strings do not play a critical role in preventing global buckling. Therefore, a small value of $\eta_P = 10^{-4}$ is used in the presented examples. Fig. 7(a) shows the contour levels of mass ratio μ_{3D} plotted for different values of angle α and complexity q. It shows a global minimum achieved at $q = 3$ and $\alpha = 31^\circ$. This optimum solution of $\mu_{3D} = 0.2159$ obtained from Fig. 7(a) has lower mass than that obtained by optimizing the pre-stress factor γ_D. The optimum configuration of the T-bar structure drawn to the scale is shown in Fig. 7(b).

Table 2
Mass ratio μ_{3D} optimized with two different approaches for different values of force f and length l. Units: f (N), l (m), and α (deg).

$\frac{f}{l^2}$	f	l	Pre-stress method				Area method			
			q	α	μ_{3D}	ϕ_{3D}	q	α	μ_{3D}	ϕ_{3D}
1000	1000	1	4	19	0.10	1.60	4	27	0.07	1.12
2500	2500	1	4	22	0.14	2.12	4	29	0.11	1.66
10000	10000	1	3	25	0.25	1.89	3	31	0.21	1.58
100000	1000	0.1	1	28	0.66	1.32	1	33	0.64	1.28
250000	2500	0.1	1	31	1.04	1.57	1	33	1.01	1.53
1000000	10000	0.1	1	36	1.56	1.56	1	33	1.54	1.54

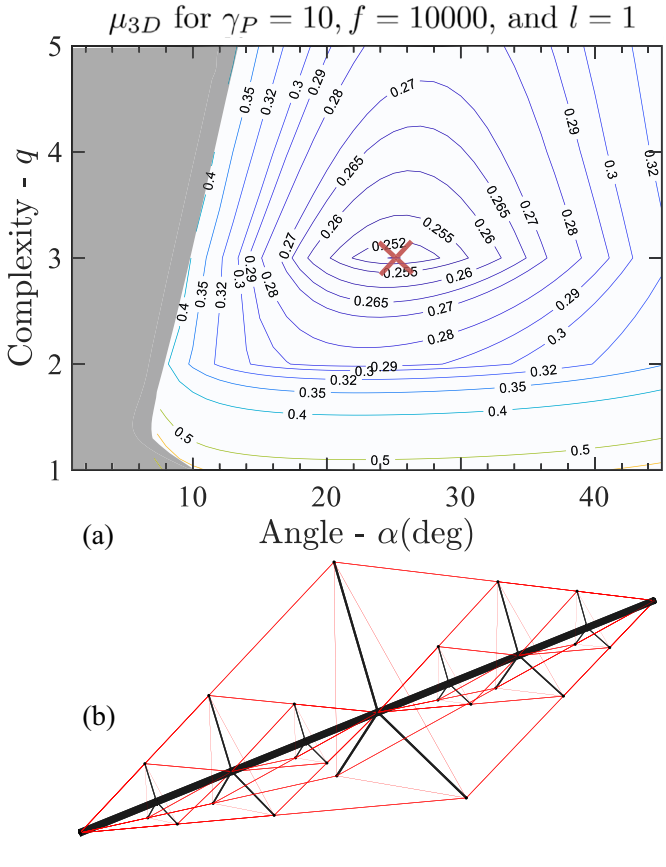

Fig. 6. (a) Contour plots of mass ratio μ_{3D} for a fixed pre-stress factor in the planar strings ($\gamma_P = 10$) and optimized pre-stress factor in diagonal strings (γ_D). (b) Optimum configuration of the T-bar structure (marked with the ' × ' in the contour) displaying calculated member cross-sections.

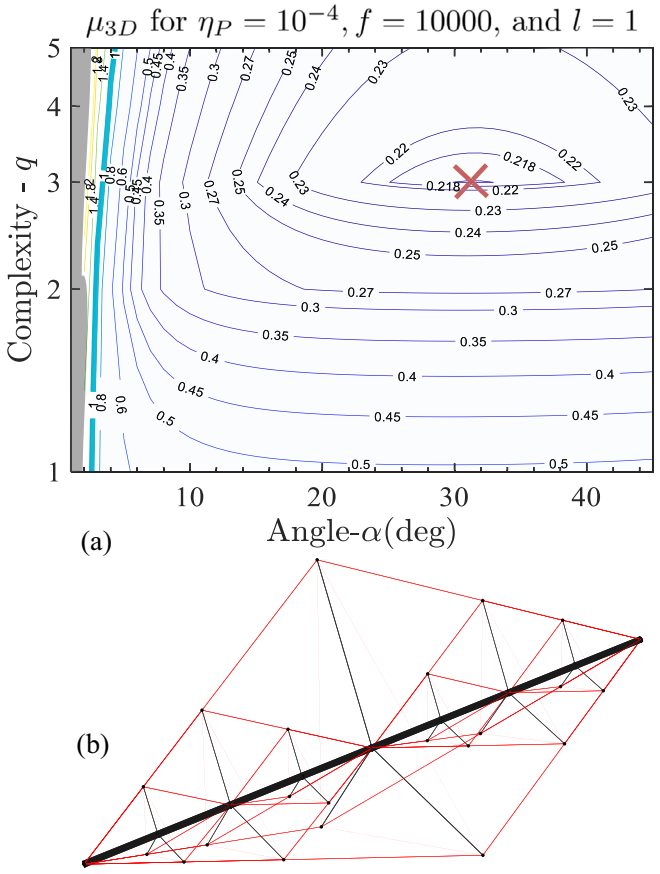

Fig. 7. (a) Contour plots of mass ratio μ_{3D} for a fixed area factor in the planar strings ($\eta_P = 10^{-4}$) and optimized area factor in diagonal strings (η_D) with different complexities q. (b) Optimum configuration of the T-bar structure (marked with the ' × ' in the contour) displaying calculated member cross-sections.

Table 2 provides the optimum α and q for different combinations of force f and length l. It is observed from the table that for all combinations of f and l, the method of optimizing area factor η_D provides lower mass solutions than those obtained by optimizing the pre-stress factor γ_D. Similar to the results observed in Table 1, the value of mass ratio μ_{3D} increases by increasing the value of f/l^2 and the mass ratio becomes greater than 1 ($\mu_{3D}(\gamma_D) = 1.0429 > 1$, $\mu_{3D}(\eta_D) = 1.0163 > 1$) for $f/l^2 = 250000$ N/m^2 where the single column is the optimal mass solution. Similar to Table 1, for $f/l^2 = 1000000$ N/m^2, the single column is designed to avoid yielding failure and thus the mass of T-bar designed to avoid only local failures would be equal to mass of the single column, $m_{T_{local}} = m_{col}$. Thus, the reason for the mass ratios $\mu_{3D} = 1.56$ (pre-stress method) and $\mu_{2D} = 1.54$ (area method) to be above 1 is entirely based on providing global stability to the structure, hence $\mu_{3D} = \phi_{3D} = 1.56$ (pre-stress method) and $\mu_{3D} = \phi_{3D} = 1.54$ (area method).

6. Conclusions

This paper presented a novel approach to design minimum mass tensegrity T-bar lattices, which can be integrated into lightweight load-bearing architectured materials. The methodology developed in this paper allows for the determination of the complexity q, aperture angle α, and pre-stress distribution or member cross-sections areas of 2D or 3D T-bar structures with minimal mass for given compressive force f and T-bar length l. In earlier work of designing minimum mass T-bar structures, only 2D T-bar structures, or T-bars limited to complexity 1, were considered.

The paper first provided an analytical solution for the mass of a T-bar structure of arbitrary shape, topology, and pre-stress distribution considering local failure modes. The pre-stress distribution or string cross-section areas are then designed such that global buckling is also prevented with minimum mass. The utilized approach to minimize the mass of complexity $q > 1$ T-bar structures was developed by sequentially designing the T-bar units introduced at each self-similar formative iteration. The examples considered for both 2D and 3D structures provided a global minimal mass T-bar design for given force f and length l. The obtained results showed that the method of optimizing the cross-section area of the strings provides lower mass designs than those obtained by optimizing the pre-stress distribution for both 2D and 3D structures.

Declaration of Competing Interest

The authors have no competing interests to declare.

Acknowledgement

E.P.H. acknowledges the start-up faculty support from the Department of Mechanical and Aerospace Engineering at the University of California, Irvine.

References

[1] Y. Chen, T. Li, F. Scarpa, L. Wang, Lattice metamaterials with mechanically tunable Poisson's ratio for vibration control, Phys. Rev. Appl. 7 (2) (2017) 24012.
[2] D.R. Reid, N. Pashine, J.M. Wozniak, H.M. Jaeger, A.J. Liu, S.R. Nagel, J.J. de Pablo, Auxetic metamaterials from disordered networks, Proc. Nat.l. Acad. Sci. 115 (7) (2018) E1384–E1390.
[3] Y. Chen, Z. Jia, L. Wang, Hierarchical honeycomb lattice metamaterials with improved thermal resistance and mechanical properties, Compos. Struct. 152 (2016) 395–402.
[4] Q. Wang, J.A. Jackson, Q. Ge, J.B. Hopkins, C.M. Spadaccini, N.X. Fang, Lightweight mechanical metamaterials with tunable negative thermal expansion, Phys. Rev. Lett. 117 (17) (2016) 175901.
[5] W. Miller, D. Mackenzie, C. Smith, K. Evans, A generalised scale-independent mechanism for tailoring of thermal expansivity: positive and negative, Mech. Mater. 40 (4–5) (2008) 351–361.
[6] X. Zheng, H. Lee, T.H. Weisgraber, M. Shusteff, J. DeOtte, E.B. Duoss, J.D. Kuntz, M.M. Biener, Q. Ge, J.A. Jackson, S.O. Kucheyev, N.X. Fang, C.M. Spadaccini, Ultralight, ultrastiff mechanical metamaterials, Science 344 (6190) (2014) 1373–1377.
[7] M. Mohsenizadeh, F. Gasbarri, M. Munther, A. Beheshti, K. Davami, Additively–manufactured lightweight metamaterials for energy absorption, Mater. Design 139 (2018) 521–530.
[8] L. Zhao, E.A. Peraza Hernandez, Theoretical study of tensegrity systems with tunable energy dissipation, Extreme Mech. Lett. 32 (2019) 100567.
[9] R. Connelly, Tensegrity structures: why are they stable? in: Rigidity Theory and Applications, Springer, 2002, pp. 47–54.
[10] F. Fraternali, G. Carpentieri, A. Amendola, R.E. Skelton, V.F. Nesterenko, Multiscale tunability of solitary wave dynamics in tensegrity metamaterials, Appl. Phys. Lett. 105 (20) (2014) 201903.
[11] Q. Zhang, D. Zhang, Y. Dobah, F. Scarpa, F. Fraternali, R.E. Skelton, Tensegrity cell mechanical metamaterial with metal rubber, Appl. Phys. Lett. 113 (3) (2018) 31906.
[12] R.E. Skelton, M.C. de Oliveira, Tensegrity Systems, Springer, 2009.
[13] R. Goyal, E.A. Peraza Hernandez, R. Skelton, Analytical study of tensegrity lattices for mass-efficient mechanical energy absorption, Int. J. Space Struct. 34 (1–2) (2019) 3–21.
[14] R.E. Skelton, M.C. de Oliveira, Optimal tensegrity structures in bending: the discrete Michell truss, J. Frankl. Inst. 347 (1) (2010) 257–283.
[15] S. Ma, X.-F. Yuan, A. Samy, Shape optimization of a new tensegrity torus, Mech. Res. Commun. 100 (2019) 103396.
[16] R. Montuori, R.E. Skelton, Globally stable tensegrity compressive structures for arbitrary complexity, Compos. Struct. 179 (2017) 682–694.
[17] D.D. Tommasi, G. Marano, G. Puglisi, F. Trentadue, Morphological optimization of tensegrity-type metamaterials, Compos. Part B 115 (2017) 182–187.
[18] F. Fraternali, A. Amendola, Mechanical modeling of innovative metamaterials alternating pentamode lattices and confinement plates, J. Mech. Phys. Solids 99 (2017) 259–271.
[19] A. Amendola, G. Carpentieri, L. Feo, F. Fraternali, Bending dominated response of layered mechanical metamaterials alternating pentamode lattices and confinement plates, Compos. Struct. 157 (2016) 71–77.
[20] A.P. Sabelhaus, J. Bruce, K. Caluwaerts, P. Manovi, R.F. Firoozi, S. Dobi, A.M. Agogino, V. SunSpiral, System design and locomotion of SUPERball, an untethered tensegrity robot, in: 2015 IEEE International Conference on Robotics and Automation (ICRA), IEEE, 2015, pp. 2867–2873.
[21] L.-H. Chen, K. Kim, E. Tang, K. Li, R. House, E.L. Zhu, K. Fountain, A.M. Agogino, A. Agogino, V. Sunspiral, E. Yung, Soft spherical tensegrity robot design using rod-centered actuation and control, J. Mech. Robot. 9 (2) (2017) 25001.
[22] G. Carpentieri, R.E. Skelton, F. Fraternali, Minimum mass and optimal complexity of planar tensegrity bridges, Int. J. Space Struct. 30 (3–4) (2015) 221–243.
[23] R. Skelton, F. Fraternali, G. Carpentieri, A. Micheletti, Minimum mass design of tensegrity bridges with parametric architecture and multiscale complexity, Mech. Res. Commun. 58 (2014) 124–132.
[24] R. Goyal, E.A. Peraza Hernandez, M. Majji, R. Skelton, Design of tensegrity structures with static and dynamic modal requirements, Proceedings of ASCE Earth and Space, to Appear, 2020.
[25] R. Goyal, R.E. Skelton, Tensegrity system dynamics with rigid bars and massive strings, Multibody Syst. Dyn. 46(3) (2019) 203–228.
[26] C.P. Johnson, K.M. Will, Beam buckling by finite element procedure, J. Struct. Divis. 100 (Proc Paper 10432) (1974).
[27] M. Mukhopadhyay, A. Mukherjee, Finite element buckling analysis of stiffened plates, Comput. Struct. 34 (6) (1990) 795–803.